Ultrafast Science
A SCIENCE PARTNER JOURNAL

REVIEW

Breakdown Spectroscopy Induced by Nonlinear Interactions of Femtosecond Laser Filaments and Multidimensional Plasma Gratings

Mengyun Hu[1,2,3], Shupeng Xu[1,2*], Shuai Yuan[2,3], and Heping Zeng[1,2,4*]

[1]State Key Laboratory of Precision Spectroscopy, East China Normal University, Shanghai 200062, China. [2]Chongqing Key Laboratory of Precision Optics, Chongqing Institute of East China Normal University, Chongqing 401120, China. [3]Shanghai Key Lab of Modern Optical System, University of Shanghai for Science and Technology, Shanghai 200093, China. [4]Jinan Institute of Quantum Technology, Jinan, China.

*Address correspondence to: spxu@lps.ecnu.edu.cn (S.X.); hpzeng@phy.ecnu.edu.cn (H.Z.)

Breakdown spectroscopy is a valuable tool for determining elements in solids, liquids, and gases. All materials in the breakdown region can be ionized and dissociated into highly excited fragments and emit characteristic fluorescence spectra. In this sense, the elemental composition of materials can be evaluated by detecting the fluorescence spectrum. This paper reviews the recent developments in laser-induced breakdown spectroscopy. The traditional laser-induced breakdown spectroscopy, filament-induced breakdown spectroscopy, plasma grating, and multidimensional plasma grating-induced breakdown spectroscopy are introduced. There are also some proposals for applications of plasma gratings, such as laser ablation, laser deposition, and laser catalysis of chemical reactions in conjunction with research on the properties of plasma gratings.

Citation: Hu M, Xu S, Yuan S, Zeng H. Breakdown Spectroscopy Induced by Nonlinear Interactions of Femtosecond Laser Filaments and Multidimensional Plasma Gratings. *Ultrafast Sci.* 2023;3:Article 0013. https://doi.org/10.34133/ultrafastscience.0013

Submitted 14 September 2022
Accepted 21 December 2022
Published 30 January 2023

Introduction

Laser-induced breakdown spectroscopy (LIBS) technology is a spectral analysis technology developed rapidly in recent years. It is a well-developed technique for efficient, precise, and multi-elemental material analysis [1,2]. When a high-energy pulse laser irradiates a material, electrons gain energy from incident photons. The atoms/molecules at the surface of samples are promoted to the excited states, giving rise to discrete spectral lines. The composition of the specimen by spectral analysis can be evaluated [3,4]. As compared with other analytical techniques such as atomic absorption spectrometry, plasma mass spectrometry, and spectrophotometry, the advantages of LIBS include direct analysis without a complex pretreatment, speedy response, and multiple elemental analysis.

For traditional LIBS systems, nanosecond (ns) pulse lasers are widely used. In the case of the conventional ns-LIBS system, an ns laser pulse from a Q-switched laser is focused upon samples, excites, and ionizes the sample. The processes of ns laser pulse inducing ionization can be concluded as follows: (a) multiphoton/tunneling ionization, which provides initial seed electrons for subsequent reactions, and (b) when the seed electrons accumulate to a particular density, avalanche ionization occurs on the ns scale (that is, within the range of ns laser irradiation), resulting in a plasma plume. In the ns-LIBS, there will be a powerful thermal effect, a plasma shielding effect, and a complicated matrix effect. As a result, low repeatability, high signal-to-noise ratios, and challenging molecular measurements are drawbacks of ns-LIBS. These shortcomings make the accuracy and sensitivity insufficient in ns-LIBS, affecting the quantitative analysis. The improvement focuses on the optimization of spectral signals, mainly to enhance the intensity of spectral signals, improve the signal-to-noise ratio, reduce matrix effects, etc. Theoretically, LIBS can be improved in terms of the laser source, material characteristics, sample structure, etc. In recent years, many assisted improvement methods have emerged, such as the enhancement of nanometal particles [5], using a metal substrate [6], gas assist [7], plasma confinement [8], etc. These methods change the structure of the tested material and have achieved good results. To obtain better fluorescence signal intensity, it is considered that 2 pulses can be used for LIBS. Hence, double-pulse LIBS (DP-LIBS) was proposed based on the consideration of multiple excitations induced by laser. The DP-LIBS mainly includes collinear (pulse delay is set to excite plasma plume twice [9]), orthogonal preablation (laser with a different pulse width can be reasonably combined to excite more signals [10]) and dual-pulse crossed beam. In the initial research, homologous double pulses were applied to the sample and enhanced the plasma density, which excites stronger spectral line signals [11,12]. Subsequent studies proposed the use of nonhomologous pulses for DP-LIBS, which again increased the spectral line signal intensity [13]. In recent research [14], DP-LIBS is combined with the absorption characteristic of the material. The released fluorescence is used to excite the target material so that DP-LIBS can be applied to the detection of more elements. With the development of ultrashort pulse laser, the emergence of picosecond (ps) and femtosecond (fs) pulse lasers has brought new vitality to LIBS technology. The pulse duration of ps or fs pulse lasers is much shorter than

that of ns pulse lasers. Thus, under the impact of short pulses, less plasma shielding effect and higher power density yield higher signal-to-background ratios and resolutions [15]. Because of the shorter pulse duration, abundant molecular fragments appeared in the breakdown region. Therefore, the fluorescence spectra of either ps-LIBS or fs-LIBS can also provide information about atoms and molecules. Meanwhile, filament-induced breakdown spectroscopy (FIBS) [16], plasma grating-induced breakdown spectroscopy (GIBS) [17], and multidimensional plasma grating-induced breakdown spectroscopy (MIBS) [18,19] were proposed recently. These new generation methods are improved from the source of excitation, which can well retain the original advantages of LIBS. The disadvantage of weak signals caused by low laser intensity is overcome by improving the excitation laser source. Moreover, through the improvement of laser intensity, the range of detected elements has been broadened, and the breadth of detection has been dramatically improved.

This article will review the progresses of techniques based on ultrafast LIBS. On the basis of the plasma grating formed by the cross nonlinear interference of beams, the induced breakdown spectroscopy of multiple beam superposition was proposed to solve the influence of the clamping effect of fs filament on the action of the material. The essence is that the nonlinear interference of time domain synchronous filament forms the plasma grating, which yields stronger fluorescence. This can be used as the secondary excitation source in DP-LIBS, such as in solution detection of LIBS. Given that certain microbubbles are produced by laser ablation and that water pressure shortens the plasma lifespan [20], a time delay beam detection technique filament and plasma grating induced breakdown spectroscopy (F-GIBS) was proposed to solve these issues. This method can perform double excitation of the sample to generate more abundant information. These studies laid the foundation for multibeam LIBS and guided the direction for the application of ultrafast laser technology.

Single Beam Induced Breakdown Detection

In 1962, 2 years after the invention of the ruby laser, the LIBS technology was proposed [21]. Induced breakdown spectroscopy has advanced along with the development of laser technology (LIBS–FIBS–GIBS–MIBS). The signal intensity, sensitivity, and limit of detection (LOD) have all substantially improved, and the usage in detection is growing. After almost 60 years of research, LIBS technology is steadily improving and becoming more practical. At present, it has been applied to soil composition analysis [22–24], water monitoring [25–27], metallurgical analysis [28,29], biomedical science [30–32], nuclear reactant detection [33,34], space exploration [35–37], and so forth.

For ns-LIBS, the excitation source is an ns laser pulse. The excitation process of materials by ns lasers (Fig. 1A) is mainly divided into the following 4 stages [38]: The first stage involves energy absorption and temperature rise. Because of the relatively long duration of the ns pulse, ongoing laser energy will raise the temperature of the material. This stage lasts up to dozens of ps. The second stage is the ablation process produced by the ns laser thermal effect. At this time, the material absorbs the laser energy and vaporization so that the material is separated from the surface, rapidly sputters, and expands outward to form plasma. In the third stage, the plasma continues to expand, which is accompanied by the formation of shock waves. In this sense, the plasma expands at supersonic speeds.

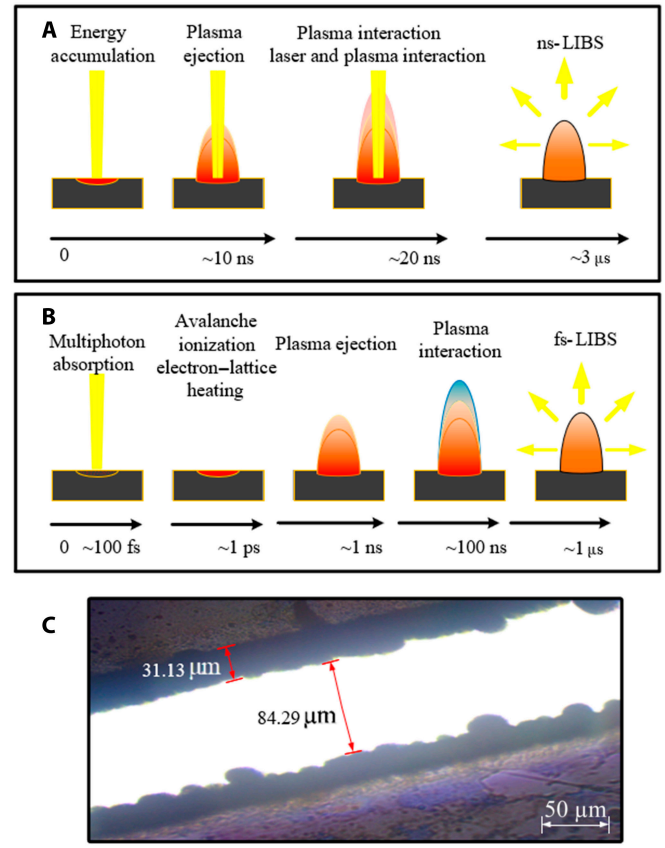

Fig. 1. (A) Generation and evolution of plasma induced by ns laser pulses. (B) Generation and evolution of plasma induced by fs laser pulses. (C) Scratching of thick 25-μm amorphous metal film by fs laser (single pulse energy of 1.3 mJ, and pulse width of 300 fs).

Finally, an expanding ellipsoid plasma appears on the outside of the material. In addition, according to the natural frequency of the material, a shock wave is formed inside the material. The plasma will continue to reach a high temperature because the ns laser pulse is still active. The fourth stage is the process of plasma radiation. At this time, the duration of the ns laser pulse ends, and the generated plasma will gradually cool down because of the outward radiation energy. At this stage, the characteristic spectral lines produced by the radiation can reflect the present elements in the material.

There is a quantitative relationship between the intensity of the radiation spectral line and the atomic concentration [39]. With the increase of laser energy density, more plasma will be excited. However, too much plasma will prevent the subsequent laser energy from acting on the surface of the sample for effective excitation, resulting in a plasma shielding effect. Different matrices will also have different degrees of excitation, which is called the matrix effect. In addition, because the electrons will be accelerated to a relatively high speed, giving rise to substantial bremsstrahlung effect, this can seriously affect the detection of the target spectrum. Fortunately, the lifetime of the continuous spectrum signal generated by bremsstrahlung is shorter than the characteristic spectral line. It is necessary to set appropriate detection delay and detection gate width in ns-LIBS to filter continuum signals. There are already many applications to demonstrate the superior performance of ns-LIBS. Over 12 elements (Cr, Si, Cu, Na, Fe, Sn, Mg, etc.) [40,41] have been reported using

LIBS detection in liquid media. However, because of surface ripples and emitted intensity extinction [42], the practical application of this method in liquid analysis has lower sensitivity and precision. To solve these difficulties, a new method based on a hydrogel solidification technique followed by LIBS analysis of liquid samples is proposed [38]. On the basis of sodium polyacrylate resin's intense water absorption properties, the hydrogel rapidly formed, and then the liquid sample can be analyzed. At the same time, a liquid LIBS analysis based on the single-drop microextraction (SDME) method was also proposed [43], and the SDME–LIBS method improved the measurement sensitivity by 2.0 to 2.6 times.

A high-energy beam is presented in a transparent atmospheric medium as filamentation results from the dynamic balance between Kerr self-focusing and plasma defocusing. [44,45]. The mechanism of action between filament and materials are illustrated in Fig. 1B. For fs laser, the intensity of a single pulse reaches 10^{10} to 10^{12} W. Therefore, it will generate a Coulomb explosion in fs-scale time, thereby generating plasma plume. Because there is no laser energy supply in the latter stage, the plasma will cool down quickly, resulting in characteristic spectral lines. Combined with the highly narrow pulse width of the fs laser, the plasma shielding effect is well resolved, which makes it suitable for depth profiling and gas composition detection. When fs laser acts on the sample's surface, the generated ablation pits are flatter [46], the surface deposition is less, and the surface damage is insignificant. Hence, it is more suitable for the field of material microprocessing detection.

In the standard scenario, altering the incident light's peak intensity and spot area can successfully alter the laser intensity. However, for fs laser filaments, it is the result of the interaction balance of internal nonlinear effects; thus, there is the intensity clamping effect. The laser power density in the filament will remain nearly constant at 5×10^{13} W/cm^2, and the electron density is also difficult to exceed 10^{17} cm^{-3} [44,47]. It reduced the influence of the laser intensity fluctuation on the spectral intensity. The long plasma channel of the filament can be regarded as a collection of a series of focal points [16,48,49]. Hence, for FIBS, the influence of the sample position relative to the lens on the spectral signal intensity is substantially reduced. The fs filament can still be effective after long-distance propagation, and the distance can reach 100 m or even kilometers [45]. Hence, FIBS technology can help implement long-distance remote sensing detection [50,51]. Kasparian et al. [52] studied the high-power fs laser pulse and observed the filament at a high altitude of more than 20 km, which paved the way for remote sensing detection. The theoretical detection distance of the system can reach more than 1.9 km. We can use this ultra-long-distance detection capability of FIBS technology in extreme environments with distance requirements such as metallurgy, nuclear fusion reaction detection, and aerospace detection. Moreover, the filament prevents the influence of the plasma shielding effect and improves the spectral intensity, signal-to-noise ratio, and resolution [53–55]. At the same time, because of the energy density of the filament having reached the order of 10^{13} W/cm^2, the influence of the matrix effect is reduced. These advantages enable FIBS technology to monitor chemical reaction processes [56,57]. At the same time, the fs filament has a high efficiency to excite the plasma. From Fig. 1C, we can see that the thermal effect produced by the Gaussian spot of filament is about 31.13 microns. The scratch width of the film material here is about 116 microns, and the cutting is very flat. This shows the advantage of no cumulative thermal effect, so FIBS can proceed the micro-loss analysis [58,59]. FIBS can deliver laser pulses over long distances. However, the plasma density and laser intensity are clamped inside a typical filament. It is a limitation for increasing the excitation field and enhancing the resolutions of spectral lines.

Fortunately, the clamping effect of laser intensity can be overcome by plasma grating induced by nonlinear interactions between multiple fs filaments [60,61]. The electron density in plasma grating has been up to be an order of magnitude higher than in filaments. Therefore, GIBS can effectively overcome the shortcomings of ns-LIBS, fs-LIBS, and FIBS.

Multibeam Interference Induced Breakdown Detection

Figure 2A shows us the basic schematic of multiple beam noncollinear coupling. Its signal intensity can be increased by more than 3 times for GIBS, and the lifetime of the plasma induced by the plasma grating is almost twice that induced by the FIBS of the same initial pulse. As shown in Fig. 2A, the beam splitter (BS1 and BS2) is used to divide the beam into 3 equal parts, and the time domain adjustment of the 3 beams can be realized by setting delays τ_1 and τ_2 to actualize the nonlinear interference of the 3 beams. The concept of using multibeam interference for induced breakdown detection mainly considers the unique effect of the nonlinear superposition of high-energy beams. The basic structure is shown in Fig. 2B. Among them, the multibeams' high-energy pulse laser and its delay can be adjusted reasonably according to the requirements. On one hand, it supplies the fundamental conditions for the multiple excitations of the material; on the other hand, it can perform the nonlinear interference of the high-energy laser beam by modifying the time domain of the beam to be consistent, thereby increasing the plasma density of the single beam and further improving the detection intensity [62]. This concept can also give guidance in various fields of laser applications, such as large area array shock peening, multibeam coupling, and phased arrays.

When two fs filaments intersect at a suitable crossing angle and the optical paths are adjusted equivalent, a fs plasma grating is formed [63,64]. The technical principle is illustrated in Fig. 2C. This source is used to excite the sample in GIBS. Plasma grating has high stability in GIBS analysis, which is due to the strong coupling of the 2 filaments. The interaction region has a certain length. The electron density and power density will maintain a relatively stable value in the plasma microchannel of this length. It also helps to reduce the influence of the sample position on the spectral line signal [17]. GIBS technology is based on fs laser technology, so it can also overcome the plasma shielding effect and matrix effect. In addition, filaments can also interact with each other to form a plasma grating after long-distance transmission. Hence, theoretically, GIBS can also realize long-distance remote sensing detection like FIBS. At present, GIBS technology is a new technology to enhance signal intensity. Furthermore, the interaction of multiple fs filaments can form multidimensional plasma gratings. In theory, it can be known that multidimensional plasma gratings are expected to achieve higher power density and electron density. Hence, it can be used in induced breakdown spectroscopy to obtain higher intensity lines.

According to nonlinear optics, the interaction of multiple filaments can produce light bullet fusion, fission, and spiraling [65–68]. The multiple high-intensity laser pulse nonlinear

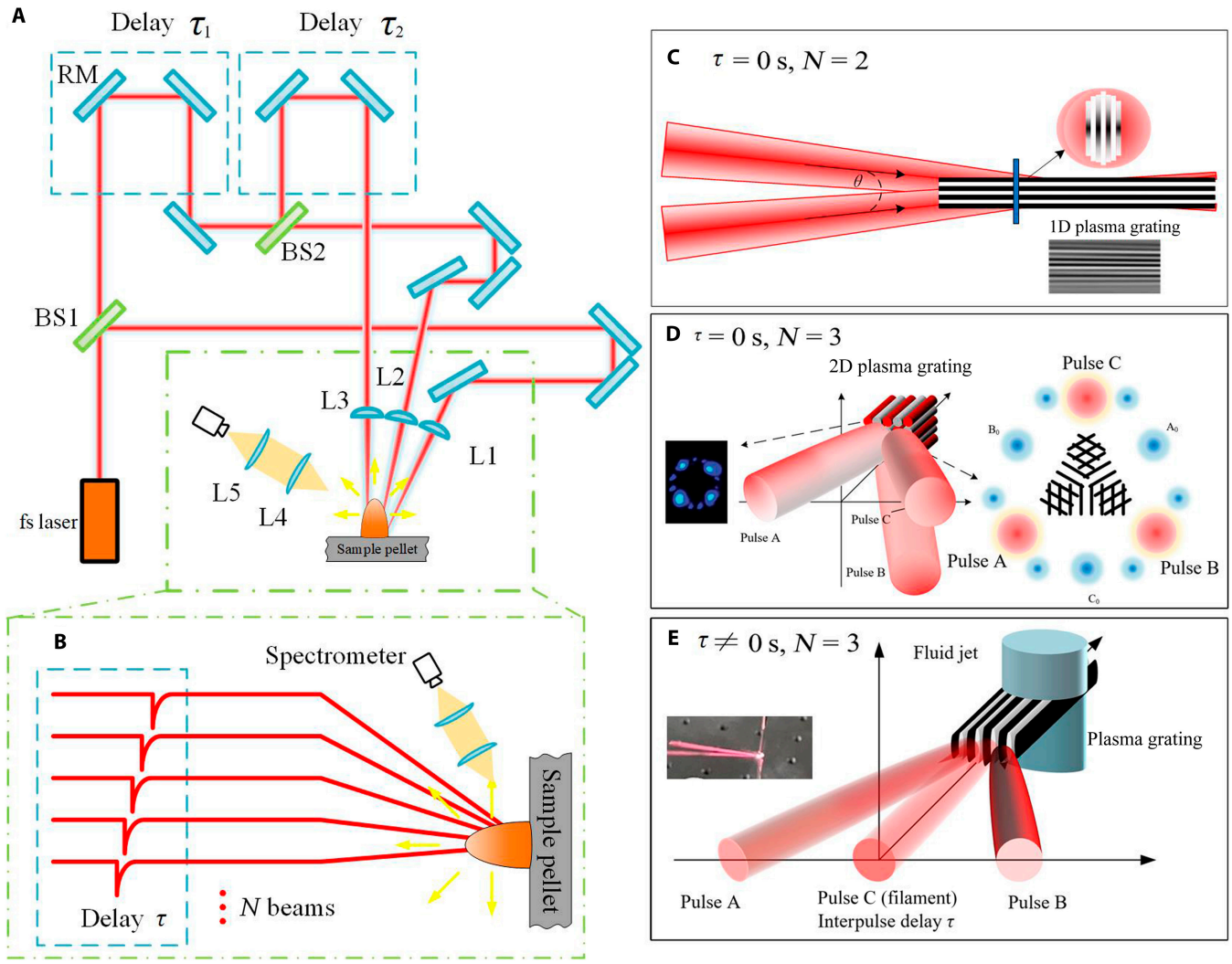

Fig. 2. (A) Basic schematic diagram of multidimensional plasma grating-induced breakdown spectroscopy (MIBS). (B) Structure multibeam laser noncollinear coupling. (C) Plasma grating structure. Inset: The interference grating fringes observed at the top. (D) Formation mechanism of multidimensional plasma grating. Inset: Three-beam interference spot. (E) The fundamentals of F-GIBS. Inset: Effect of fs-laser and fluid jet with no delay.

interference can make the power density of the laser exceed the limit of clamping. Previous studies have shown that the spatial modulation of 2 filaments can form a 1-dimensional periodic plasma grating with a spatial period of several tens of microns [69,70]. Experiments show that the mutual overlapping of 3 filaments can produce multidimensional plasma grating, which can be considered relatively high-intensity pulses applied for high optical damage thresholds. In this spatial structure, a substantial enhancement of the third harmonic can be observed, as well as the transfer of energy between filaments. In addition, the basic structure of a 3-beam generated plasma grating can be seen in Fig. 2D.

The multidimensional plasma grating produced by the interference of 3 fs filaments can be an excellent excitation source for trace detection of heavy metals in soil. Therefore, MIBS was proposed in the study [18], and it was observed that the signal intensity of MIBS was 2 times that of GIBS, and the induced plasma lifetime of MIBS was also increased by about 20%. It can be observed in Fig. 3 that the clamped power density of the multidimensional plasma grating structure is about 1.67 times that of the plasma grating structure. The higher the clamping intensity, the higher the plasma energy and the higher the detection signal. At the same time, it can also be observed that the clamping power density will decrease after the delay of the 3 beams is introduced. However, it is still higher than that of the plasma grating structure. As the delay increases, the third beam plays the role of regenerating the plasma grating, which gives the subsequent development of F-GIBS a theoretical basis.

In order to see the influence of plasma grating on the excitation fluorescence spectral line, in Fig. 4, we compared the changes of the spectral lines in the air of multibeam coupled excitation under different energies. With the increased laser pulse energy, the fluorescence spectrum waveform induced by a single filament in the air almost did not change, but the relative intensity increased (Fig. 4A). This means that the single filament is limited by the clamping effect. For GIBS, the variation of fluorescence spectrum waveform can be observed when the pulse energy reaches 0.8 mJ (Fig. 4B). For MIBS, it is already observed when the energy is about 0.4 mJ, and this phenomenon becomes more pronounced with increasing energy (Fig. 4C). This variation is associated with supercontinuum spectroscopy. The power of multifilament coupling in the air induces the ionized

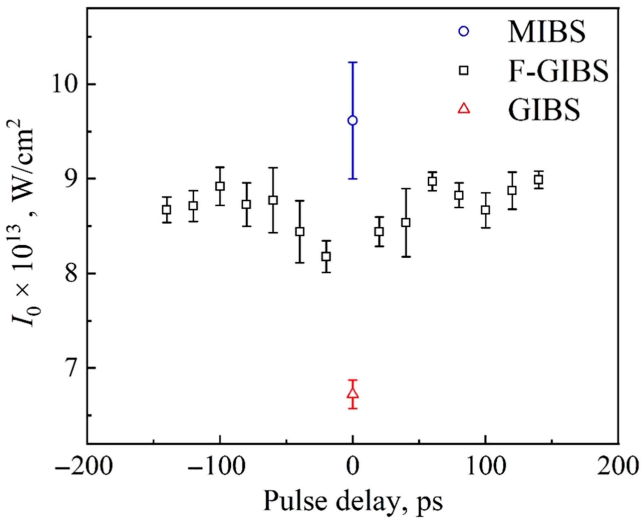

Fig. 3. The intensity clamping in air. For MIBS, there is the multidimensional plasma grating. For F-GIBS, there is the nonlinear interference of the 3 filaments, in which the time domain of the 2 filaments is synchronized and the time domain of the third filament is delayed from the previous filament. For GIBS, there is the plasma grating formed by nonlinear interference.

air fluorescence to appear obvious supercontinuum phenomenon. In the comparison of the 3 cases in Fig. 4D, under the total pulse energy of 1 mJ, the relative intensity of the fluorescence excited by the plasma grating is much larger than the single filament, showing the superiority of the multibeam nonlinear interference-induced breakdown spectroscopy.

Inheriting the theory of MIBS, the multidimensional plasma grating improves the signal intensity of detection. Still, there is no acceptable solution to the side effects of violent plasma explosion and bubbles in the liquid detection mechanism. Therefore, combining the primary theories of FIBS, GIBS, and MIBS, the coplanar interaction of multiple filaments is intentionally used to effectively control the plasma expansion and formation of bubbles in the fluid. Two filaments form a 1-dimensional plasma grating, like GIBS. In this situation, we can use another fs filament, which has an individual delay from the first 2 filaments that form the plasma grating, to achieve the combination of FIBS and GIBS, as shown in Fig. 2E. Because the third filament and plasma grating are appropriately delayed or synchronized on the fluid jet, their nonlinear interaction enhances plasma excitation and prolongs plasma lifetime. A conceptually distinct dual-pulse excitation, F-GIBS is established. It produces a

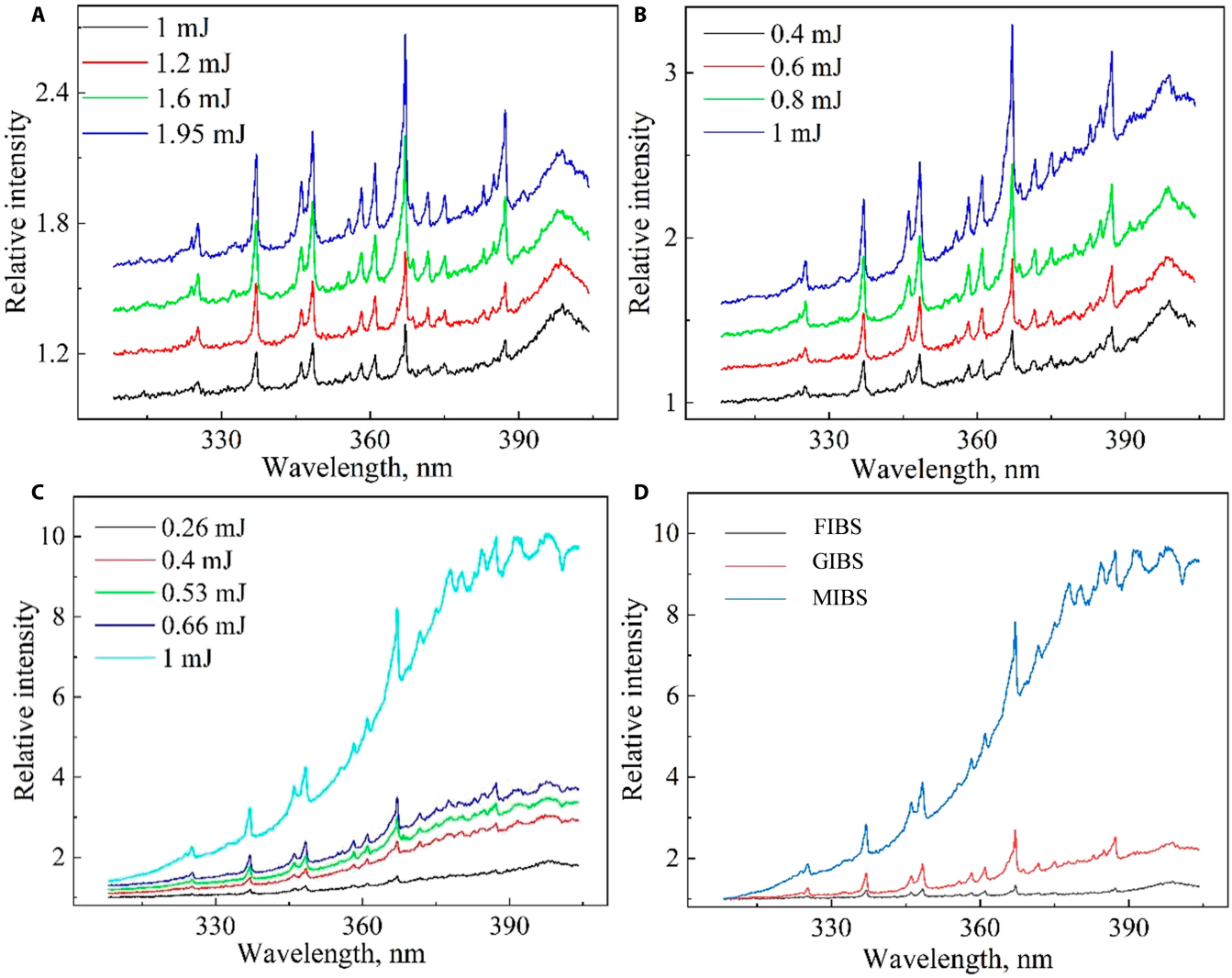

Fig. 4. Fluorescence spectra excited in air by fs laser pulses of different energies. (A) FIBS. (B) GIBS. (C) MIBS. (D) Comparing of the fluorescence spectra when the total laser pulse energy reaches 1 mJ.

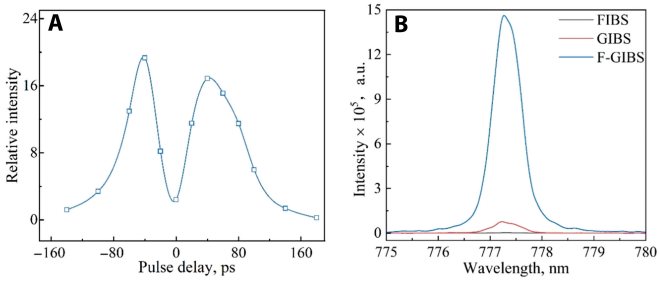

Fig. 5. (A) The change of relative intensity obtained by F-GIBS at the interpulse delay. (B) Comparison of FIBS, GIBS, and F-GIBS in aqueous solutions for spectral lines of O I 777.2-nm elements, and F-GIBS with pulse delay of −50 ps. a.u., arbitrary units.

Table 1. The progress of development for FIBS, GIBS, and MIBS. (The chosen spectral line: Si I 288.2 nm. The concentration of SiO_2 in the soil samples: for GSS-08, 58.61 ± 0.13 μg/g; for GSS-09, 61.09 ± 0.33 μg/g.)

In soil: for Si I 288.2 nm	FIBS [17] (sample GSS-08)	GIBS [17] (sample GSS-08)	MIBS [18] (sample GSS-09)
Intensity	1×10^4	3.2×10^4	10×10^4
Min. pulse energy	1.1 mJ	0.4 mJ	0.3 mJ
Signal duration	100 ns	200 ns	350 ns

breakdown line that is much stronger than the plasma grating and the filament alone. The experimental setup adjusts the optical path length of the third filament so that it is delayed in the time domain of the plasma grating. Three coplanar filaments construct a liquid jet with a short delay. When the third filament coincides with the plasma grating in time domain, all 3 synchronized pulses are disturbed to create a new multidimensional plasma grating, which is the interference superposition of noncollinear filaments. Given the problems with liquid testing, the obtained spectral line intensities are similar to the result of F-GIBS with large delay (see Fig. 5A). At positive delays, the third filament is ahead of plasma grating in the time domain, the delayed third pulse is filamented along the formed plasma grating, and the excitation of the plasma grating is elongated. While at negative delays, plasma grating from 2 synchronized pulses was present before plasma expansion and established an advanced plasma modulated for plasma grating. F-GIBS proved to be an effective technique for the sensitive detection of elements in liquid. From the change of the relative intensity of the spectral line signal under different delays (Fig. 5A), we can see that the delay correspondingly overcomes violent plasma explosion and the side effects of air bubbles in liquids, showing the potential of F-GIBS to detect heavy metal elements in aqueous solutions with higher sensitivity.

Because of the nonlinear interference of the filament in liquid, the energy of plasma grating can be focused on the shorter length. It plays an essential role in overcoming the influence of the water distance formed by some bubbles, as well as the sputtering effect after the laser deals with the liquid medium. This method improves the spectral signal intensity and reduces the fluctuation of the spectral signal, which provides the conditions for quantitative detection in solution. In Fig. 5B, the spectral intensities for spectral lines of O I 777.2 nm obtained by FIBS, GIBS, and F-GIBS in solution are compared. The results show that F-GIBS signal sensitivity is substantially improved.

The Development Process of Induced Breakdown Spectroscopy Based on Nonlinear Laser Theory

The variation in the signal intensity of different element spectral lines is one of the most prominent indicators of the progress for LIBS. By enhancing the detection signal intensity, LIBS can provide a broader space for applications. The application of multibeam nonlinear coupling in induced breakdown spectroscopy is a series of tremendous advances. The changes in the signal intensity of the Si I 288.2-nm spectral line for the detection of soil are shown in Table 1. At the same time, there also shows the progress of minimum laser pulse energy for the appearance of visible signals and signal duration on account of technological improvement. From these parameters, it is clear to see the advancement of technology and the superiority of GIBS and MIBS.

To accomplish the objective of quantitative analysis, it is necessary to improve the signal strength, detection sensitivity, and signal stability. The application of multibeam nonlinear coupling of fs laser to LIBS provides a direction for achieving this goal. In the LIBS, the plasma excited by an ns laser needs to be stable for detection. The delay is probably on the order of microseconds, so there is an unavoidable thermal effect. FIBS substantially reduces the thermal effect. Another advantage is that FIBS overcomes the plasma shielding effect. The original LIBS requires a plasma expansion to reach an equilibrium state for detection due to the plasma shielding effect. To further improve the measurement effect of FIBS, it is demanded to overcome the intensity clamping effect and the trouble from some different gas effects and Kerr's self-focusing. Then, GIBS has apparent advantages. In addition for MIBS, it is obvious to improve the sensitivity further. At the same time, by using GIBS technology, the ionization and decomposition of unusual materials can be achieved. The GIBS effectively weakens the influence of the matrix effect. Therefore, GIBS technology can also be used as a detection analysis for samples that are difficult to melt, decompose, and have complex substrates. MIBS further improves the 1-dimensional plasma grating to a 2-dimensional state, and the compression of the channel of plasma is better. Figure 6 shows us the development process of induced breakdown spectroscopy based on plasma grating and introduces the development direction. The nonlinear coupling of multiple beams can realize the regeneration and splicing of plasma gratings. The asynchronous coupling can realize multiple excitations. Therefore, as shown in Fig. 6, in the following research, it is considered to realize the special requirements by multibeam coupling and multiexcitation.

The progress made by LIBS is reflected by the change in the LOD. In metal material detection, LOD for Fe in the aluminum alloy reaches 9.71 parts per million (ppm) by LIBS [71]. Various methods can be used to enhance the LIBS's measurement precision

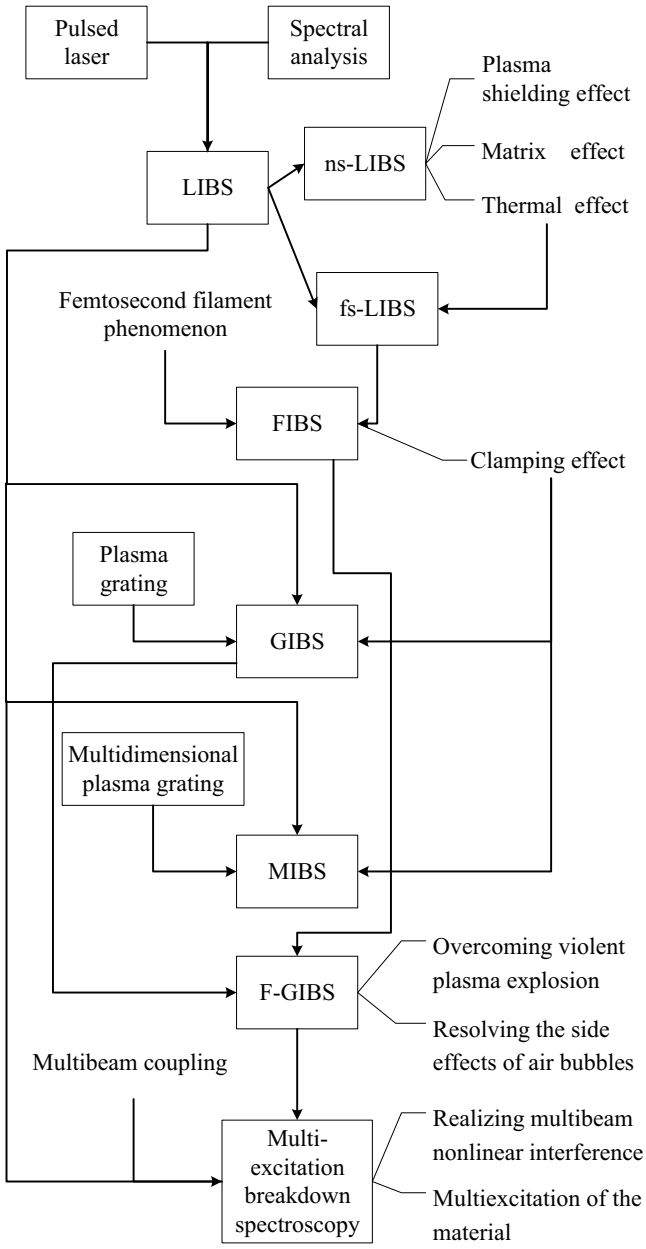

Fig. 6. The development process of breakdown spectroscopy.

when detecting liquids. For example, by combining LIBS with other measurements: time-resolved spectral image laser-induced breakdown spectroscopy (TRSI-LIBS); and by changing the form of the material: hydrogel-based solidification method (HBSM-LIBS) and SDME-LIBS. Then, with the emergence of FIBS, GIBS, and MIBS, the signal can also be observed for some materials that are difficult to excite spectral lines. In [18], the LOD for Mn in the soil was approximately 394.4 ppm by GIBS; it reached 306.47 ppm by MIBS, and the detection accuracy increased by 30% (see Table 2 for more information about LOD).

With the improvement of GIBS and MIBS about LOD, multibeam and multiexcitation appeared with a substantial improvement in induced breakdown spectroscopy technology. The study on the multibeam nonlinear interference principle will achieve excellent result in the field of induced breakdown spectroscopy.

Applications of Plasma Grating and Multidimensional Plasma Grating

Through the plasma grating and multidimensional plasma grating, the increase of filament energy and the striped spatial structure are realized in air. This provides a strong guarantee for developing the application of the laser. Here is a brief overview of the applications of these laser techniques in surface deposition, laser ablation, and chemical reactions.

With the maturity of high-energy pulsed laser technology, people gradually recognize and accept the characteristics of pulsed laser deposition (PLD). PLD is to focus the high-intensity pulsed laser beam on the surface of the target material to generate high temperature ($T \geq 10^4$ K) and ablation [76] and further create high-pressure plasma. This plasma expansion emits and deposits on the substrate to form a thin film. Typically, it can be divided into 3 processes (Fig. 7A): laser surface ablation and plasma

Table 2. The variation of LODs for different induced breakdown spectroscopy types.

Breakdown spectroscopy types		Limit of detection (LOD)
LIBS	DP-LIBS	In oil: LODs for Fe from 4 to 3 μg/g [72].
	TRSI-LIBS	In milk: LODs for Ca from 1.47 to 0.81 mg/g, accuracy increased by 57.89% [73].
	HBSM-LIBS	In water: LODs for Al from 15 to 0.46 μg/ml, for Cu From 12 to 4.69 μg/ml, and for Cr from 30 to 4.44 μg/ml [38].
	SDME-LIBS	In water: LODs for Zn from 49 to 21 μg/kg, for Mn from 427 to 301 μg/kg, for Cu from 141 to 54 μg/kg, and for Cr from 143 to 50 μg/kg [43].
	Different spectrometers	In oil: By Echelle, LODs for Fe from 4 to 3.73 μg/g. By Czerny–Turner, LODs for Fe from 4 to 2.05 μg/g [74].
FIBS		In water: LODs for Fe from 10 mg/l by LIBS to 2.6 mg/l by FIBS [75].
GIBS		Compared with the FIBS, the spectral line signal obtained by the GIBS was successfully increased by 2 to 3 times [17]. In soil: LODs for Mn [18], approximately 394.4 ppm.
MIBS		In soil: LODs for Mn [18], approximately 306.47 ppm.

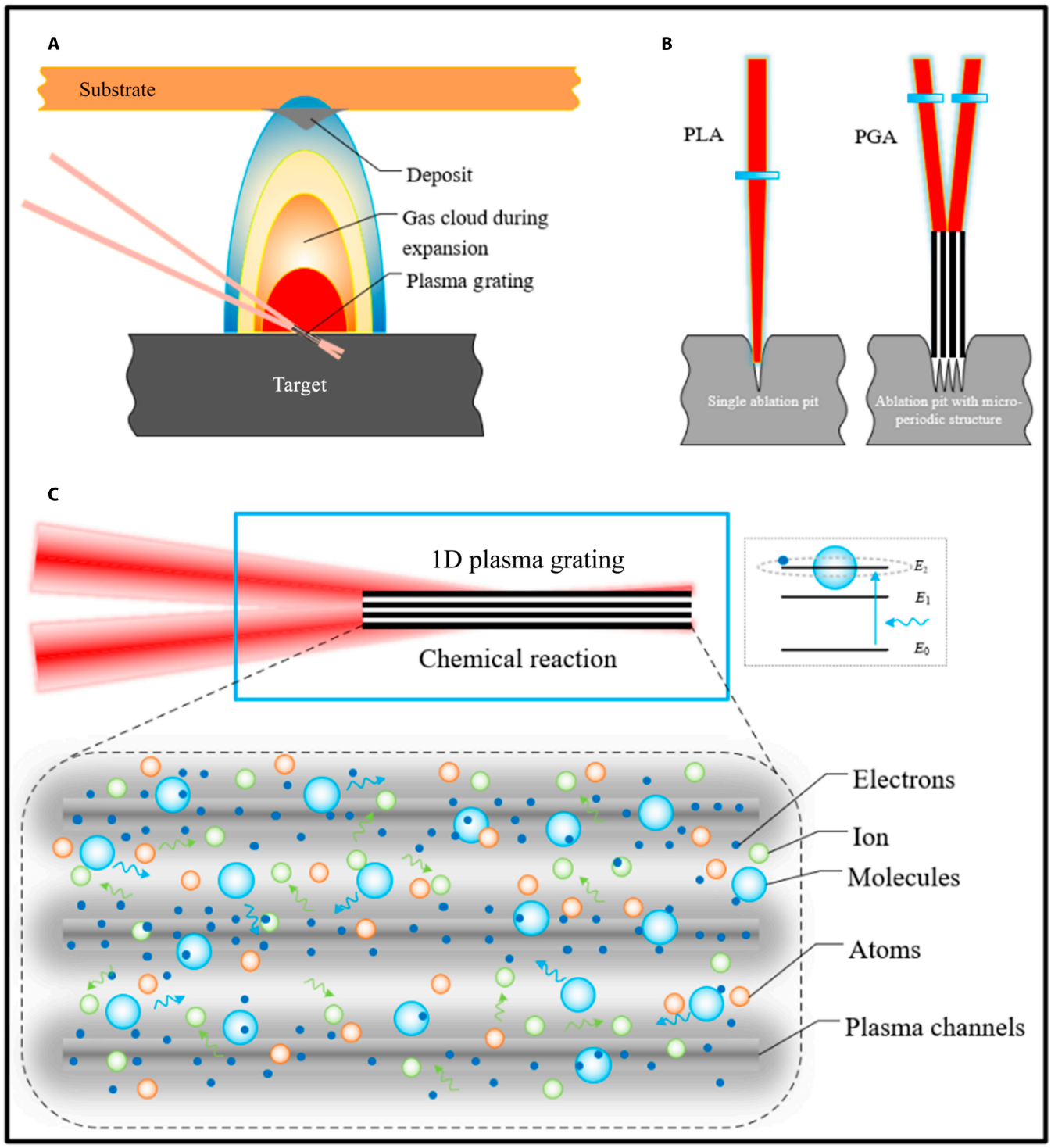

Fig. 7. (A) Basic schematic of plasma grating deposition (PGD). (B) Single ablation pit from pulsed laser ablation (PLA) and striped structure obtained by plasma grating ablation (PGA). (C) Chemical reactions induced by plasma grating.

generation, expansion and emission of plasma, and condensation and film formation on the substrate surface. The unique physical process of PLD has the following advantages compared to other film-making techniques: (a) PLD has a wide range of applications. It has been widely used in the deposition of 2-dimensional thin-film materials [77–81]. In addition, it also shows excellent compatibility on different substrates [82]. (b) It is suitable for the deposition of multicomponent compounds [83,84]. (c) Low deposition temperature [85]. (d) It is convenient to achieve the growth of multilayer films and superlattices.

In this study [86], it was found that the film with good precision, strong bonding force, and high epitaxial orientation can be deposited by fs pulse laser. Here, the fs laser pulse high-intensity characteristic is mainly applied. Therefore, considering that the clamped intensity can be promoted by the multidimensional plasma grating, the plasma grating deposition (PGD) and

multidimensional plasma grating deposition (PMD) are raised. Theoretically, they get better deposition, including the deposition faster and finer, high efficiency, the sedimentary layer smoother, and the structure more diverse.

Moreover, the ultrahigh intensity and electron density in both plasma grating can ablate materials with high damaging threshold and etched the regular fringe structure (Fig. 7B). In the plasma grating constructed from a laser with a pulse width of 300 fs and a single pulse energy of 2.8 mJ, the temperature easily exceeds 5,000 K. Hence, plasma grating ablation (PGA) and multidimensional plasma grating ablation (MGA) can be attempted to ablate the diamond (melting point of 3,773 K) and carborundum (melting point of 2,973 K). Moreover, periodical structures can be generated in nano-machining by employing the filaments at the interaction region of plasma grating. This structure can fabricate Bragg volume grating and antireflection coating of silicon solar cells.

Additionally, it results in higher resolutions of molecule tracing and opens new possibilities for substantial chemical reactions (Fig. 7C). The reason is that more vigorous field intensity and full collision of particles can break more chemical bonds, creating more dissociation and reaction channels. It finally helps us investigate the detailed dynamics of chemical reactions.

Summary

From ns to fs, from beams to filaments, from single filaments to nonlinear plasma gratings, and finally to triple filament asynchronous noncollinear coupling, it brings us an advance in breakdown spectroscopy detection from LIBS to F-GIBS. These fluorescence techniques have been successfully applied to identify various samples in the laboratory and outdoor environments with high sensitivity and a good signal-to-noise ratio. In this process, we resolve the influence of the matrix effect, plasma shielding effect, difficulty in long-distance detection, and intensity clamping effect on the detection of induced breakdown spectroscopy. Recent results on GIBS and MIBS are emphasized. The applications of these techniques confirm reliability and feasibility. At the same time, the combination of multibeam coupling in the laser field and the breakthrough progresses of substantial area array laser shock research also provides more development inspiration for the higher sensitivity and more comprehensive application range of our induced breakdown spectroscopy detection. Moreover, recent developments in both GIBS and MIBS have also opened new possibilities for film fabrication and nano-machining. The detailed dynamics of the ionization/dissociation processes and chemical reactions are yet to be explored. In this sense, there are still many challenges for practical applications and understanding the underlying physics.

Acknowledgments

Funding: This work was sponsored by Shanghai Rising-Star Program (22QC1401000), National Defense Administration of Science, Technology and Industry (HTKJ2021KL504014), National Key Research and Development Program (2018YFB0504400), National Natural Science Foundation of China (11621404, 11727812, and 62035005), and Shanghai Municipal Science and Technology Major Project (2019SHZDZX01-ZX05).

References

1. Arca G, Ciucci A, Palleschi V, Rastelli S, Tognoni E. Trace element analysis in water by the laser-induced breakdown spectroscopy technique. *Appl Spectrosc*. 1997;51(8):1102–1105.
2. Senesi GS, Harmon RS, Hark RR. Field-portable and handheld laser-induced breakdown spectroscopy: Historical review, current status and future prospects. *Spectrochim Acta B At Spectrosc*. 2021;175:Article 106013.
3. Harmon RS, Senesi GS. Laser-induced breakdown spectroscopy—A geochemical tool for the 21st century. *Appl Geochem*. 2021;128:Article 104929.
4. Legnaioli S, Campanella B, Poggialini F, Pagnotta S, Harith MA, Abdel-Salam ZA, Palleschi V. Industrial applications of laser-induced breakdown spectroscopy: A review. *Anal Methods*. 2020;12(8):1014–1029.
5. Wang M, Jiang L, Wang S, Guo Q, Tian F, Chu Z, Zhang J, Li X, Lu Y. Multiscale visualization of colloidal particle lens array mediated plasma dynamics for dielectric nanoparticle enhanced femtosecond laser-induced breakdown spectroscopy. *Anal Chem*. 2019;91(15):9952–9961.
6. Aguirre MA, Legnaioli S, Almodóvar F, Hidalgo M, Palleschi V, Canals A. Elemental analysis by surface-enhanced laser-induced breakdown spectroscopy combined with liquid–liquid microextraction. *Spectrochim Acta B At Spectrosc*. 2013;79–80:88–93.
7. Dikshit V, Yueh FY, Singh JP, McIntyre DL, Jain JC, Melikechi N. Laser induced breakdown spectroscopy: A potential tool for atmospheric carbon dioxide measurement. *Spectrochim Acta B At Spectrosc*. 2012;68:65–70.
8. Hussain A, Iqbal ST, Shahbaz RM, Zafar M, Arshad AA, Aslam K, Mukhtar M. Varying magnetic field strength as an effective approach to boost up the plasma signal in laser-induced breakdown spectroscopy. *Heliyon*. 2022;8(9):Article e10563.
9. Yueh FY, Kumar A, Singh JP. Double-pulse laser-induced breakdown spectroscopy with liquid jets of different thicknesses. *Appl Opt*. 2003;42(30):6047–6051.
10. Carter JC, Pender J, Colston BW, Chance Carter J, Michael Angel S. Dual-pulse laser-induced breakdown spectroscopy with combinations of femtosecond and nanosecond laser pulses. *Appl Opt*. 2003;42(30):6099–6106.
11. de Giacomo A, Dell'aglio M, Colao F, Fantoni R, Lazic V. Double-pulse LIBS in bulk water and on submerged bronze samples. *Appl Surf Sci*. 2005;247(1–4):157–162.
12. Bertolini A, Carelli G, Francesconi F, Marchesini L, Marsili P, Sorrentino F, Cristoforetti G, Legnaioli S, Palleschi V, Pardini L, et al. Modì: A new mobile instrument for in situ double-pulse LIBS analysis. *Anal Bioanal Chem*. 2006;385(2):240–247.
13. Elnasharty IY, Doucet FR, Gravel JFY, Bouchard P, Sabsabi M. Double-pulse LIBS combining short and long nanosecond pulses in the microjoule range. *J Anal At Spectrom*. 2014;29(9):1660–1666.
14. Pardede M, Lie TJ, Iqbal J, Bilal M, Hedwig R, Ramli M, Khumaeni A, Budi WS, Idris N, Abdulmadjid SN, et al. H-D analysis employing energy transfer from metastable excited-state He in double-pulse LIBS with low-pressure He gas. *Anal Chem*. 2019;91(2):1571–1577.
15. Giannakaris N, Haider A, Ahamer CM, Grünberger S, Trautner S, Pedarnig JD. Femtosecond single-pulse and orthogonal double-pulse laser-induced breakdown spectroscopy (LIBS): Femtogram mass detection and chemical imaging with micrometer spatial resolution. *Appl Spectrosc*. 2022;76(8):926–936.

16. Yeak J, Phillips MC, Harilal SS. Plasma temperature clamping in filamentation laser induced breakdown spectroscopy. *Opt Express*. 2015;23(21):27113–27122.
17. Hu M, Peng J, Niu S, Zeng H. Plasma-grating-induced breakdown spectroscopy. *Adv Photon*. 2020;2(6):Article 065001.
18. Hu M, Shi S, Yan M, Wu E, Zeng H. Femtosecond laser-induced breakdown spectroscopy by multidimensional plasma grating. *J Anal At Spectrom*. 2022;37(4):841–848.
19. Liu J, Li W, Pan H, Zeng H. Two-dimensional plasma grating by non-collinear femtosecond filament interaction in air. *Appl Phys Lett*. 2011;99(15):Article 151105.
20. Zhang DC, Hu ZQ, Su YB, Hai B, Zhu XL, Zhu JF, Ma X. Simple method for liquid analysis by laser-induced breakdown spectroscopy (LIBS). *Opt Express*. 2018;26(14):Article 18794.
21. Baudelet M, Smith BW. The first years of laser-induced breakdown spectroscopy. *J Anal At Spectrom*. 2013;28(5):624–629.
22. Xu X, Du C, Ma F, Shen Y, Zhou J. Forensic soil analysis using laser-induced breakdown spectroscopy (LIBS) and Fourier transform infrared total attenuated reflectance spectroscopy (FTIR-ATR): Principles and case studies. *Forensic Sci Int*. 2020;310:Article 110222.
23. Villas-Boas PR, Franco MA, Martin-Neto L, Gollany HT, Milori DMBP. Applications of laser-induced breakdown spectroscopy for soil analysis, part I: Review of fundamentals and chemical and physical properties. *Eur J Soil Sci*. 2020;71(5):789–804.
24. Villas-Boas PR, Franco MA, Martin-Neto L, Gollany HT, Milori DMBP. Applications of laser-induced breakdown spectroscopy for soil characterization, part II: Review of elemental analysis and soil classification. *Eur J Soil Sci*. 2020;71(5):805–818.
25. Contreras V, Valencia R, Peralta J, Sobral H, Meneses-Nava MA, Martinez H. Chemical elemental analysis of single acoustic-levitated water droplets by laser-induced breakdown spectroscopy. *Opt Lett*. 2018;43(10):2260–2263.
26. Tang Z, Hao Z, Zhou R, Li Q, Liu K, Zhang W, Yan J, Wei K, Li X. Sensitive analysis of fluorine and chlorine elements in water solution using laser-induced breakdown spectroscopy assisted with molecular synthesis. *Talanta*. 2020;224:Article 121784.
27. Rehan I, Gondal MA, Aldakheel RK, Rehan K, Sultana S, Almessiere MA, Ali Z. Development of laser induced breakdown spectroscopy technique to study irrigation water quality impact on nutrients and toxic elements distribution in cultivated soil. *Saudi J Biol Sci*. 2021;28(12):6876–6883.
28. Wang P, Li N, Yan C, Feng Y, Ding Y, Zhang T, Li H. Rapid quantitative analysis of the acidity of iron ore by the laser-induced breakdown spectroscopy (LIBS) technique coupled with variable importance measures-random forests (VIM-RF). *Anal Methods*. 2019;11(27):3419–3428.
29. Álvarez J, Velásquez M, Sandoval-Muñoz C, Castillo RP, Bastidas CY, Luarte D, Sbárbaro D, Rammlmair D, Yáñez J. Improved mineralogical analysis in copper ores by laser-induced breakdown spectroscopy. *J Anal At Spectrom*. 2022;37(10):1994–2004.
30. Baudelet M, Guyon L, Yu J, Wolf J-P, Amodeo T, Fréjafon E, Laloi P. Spectral signature of native CN bonds for bacterium detection and identification using femtosecond laser-induced breakdown spectroscopy. *Appl Phys Lett*. 2006;88(6):Article 063901.
31. Baudelet M, Yu J, Bossu M, Jovelet J, Wolf J-P, Amodeo T, Fréjafon E, Laloi P. Discrimination of microbiological samples using femtosecond laser-induced breakdown spectroscopy. *Appl Phys Lett*. 2006;89(16):Article 163903.
32. Chu Y, Zhang Z, He Q, Chen F, Sheng Z, Zhang D, Jin H, Jiang F, Guo L. Half-life determination of inorganic-organic hybrid nanomaterials in mice using laser-induced breakdown spectroscopy. *J Adv Res*. 2020;24:353–361.
33. Wachter JR, Cremers DA. Determination of uranium in solution using laser-induced breakdown spectroscopy. *Appl Spectrosc*. 1987;41(6):1042–1048.
34. Nakanishi R, Saeki M, Wakaida I, Ohba H. Detection of gadolinium in surrogate nuclear fuel debris using fiber-optic laser-induced breakdown spectroscopy under gamma irradiation. *Appl Sci*. 2020;10(24):Article 8985.
35. Lanza NL, Wiens RC, Clegg SM, Ollila AM, Humphries SD, Newsom HE, Barefield JE. Calibrating the ChemCam laser-induced breakdown spectroscopy instrument for carbonate minerals on Mars. *Appl Opt*. 2010;49(13):C211–C217.
36. Knight AK, Scherbarth NL, Cremers DA, Ferris MJ. Characterization of laser-induced breakdown spectroscopy (LIBS) for application to space exploration. *Appl Spectrosc*. 2000;54(3):331–340.
37. Liu C, Ling Z, Zhang J, Wu Z, Bai H, Liu Y. A stand-off laser-induced breakdown spectroscopy (LIBS) system applicable for Martian rocks studies. *Remote Sens*. 2021;13(23):Article 4773.
38. Lin Q, Bian F, Wei Z, Wang S, Duan Y. A hydrogel-based solidification method for the direct analysis of liquid samples by laser-induced breakdown spectroscopy. *J Anal At Spectrom*. 2017;32(7):1412–1419.
39. Aragón C, Aguilera JA, Peñalba F. Improvements in quantitative analysis of steel composition by laser-induced breakdown spectroscopy at atmospheric pressure using an infrared Nd:YAG laser. *Appl Spectrosc*. 1999;53(10):1259–1267.
40. Shi H, Zhao N, Wang C, Lu CP, Liu LT, Chen D, Ma MJ, Zhang YJ, Liu JG, Liu WQ. Study on measurement of trace heavy metal Ni in water by laser induced breakdown spectroscopy technique. *Spectrosc Spectr Anal*. 2012;32(1):25–28.
41. Fichet P, Mauchien P, Wagner JF, Moulin C. Quantitative elemental determination in water and oil by laser induced breakdown spectroscopy. *Anal Chim Acta*. 2001;429(2):269–278.
42. de Giacomo A, de Bonis A, Dell'Aglio M, de Pascale O, Gaudiuso R, Orlando S, Santagata A, Senesi GS, Taccogna F, Teghil R. Laser ablation of graphite in water in a range of pressure from 1 to 146 atm using single and double pulse techniques for the production of carbon nanostructures. *J Phys Chem C*. 2011;115(12):5123–5130.
43. Aguirre MA, Nikolova H, Hidalgo M, Canals A. Hyphenation of single-drop microextraction with laser-induced breakdown spectrometry for trace analysis in liquid samples: A viability study. *Anal Methods*. 2015;7(3):877–883.
44. Chin SL, Wang T-J, Marceau C, Wu J, Liu JS, Kosareva O, Panov N, Chen YP, Daigle JF, Yuan S, et al. Advances in intense femtosecond laser filamentation in air. *Laser Phys*. 2012;22(1):1–53.
45. Couairon A, Mysyrowicz A. Femtosecond filamentation in transparent media. *Phys Rep*. 2007;441(2–4):47–189.
46. Yong J, Yang Q, Hou X, Chen F. Nature-inspired superwettability achieved by femtosecond lasers. *Ultrafast Sci*. 2022;2022:Article 9895418.
47. Eisenmann S, Pukhov A, Zigler A. Fine structure of a laser-plasma filament in air. *Phys Rev Lett*. 2007;98(15):Article 155002.

48. Brodeur A, Chien CY, Ilkov FA, Chin SL, Kosareva OG, Kandidov VP. Moving focus in the propagation of ultrashort laser pulses in air. *Opt Lett*. 1997;22(5):304–306.
49. Judge EJ, Heck G, Cerkez EB, Levis RJ. Discrimination of composite graphite samples using remote filament-induced breakdown spectroscopy. *Anal Chem*. 2009;81(7):2658–2663.
50. Braun A, Korn G, Liu X, du D, Squier J, Mourou G. Self-channeling of high-peak-power femtosecond laser pulses in air. *Opt Lett*. 1995;20(1):73–75.
51. Stelmaszczyk K, Rohwetter P, Méjean G, Yu J, Salmon E, Kasparian J, Ackermann R, Wolf JP, Wöste L. Long-distance remote laser-induced breakdown spectroscopy using filamentation in air. *Appl Phys Lett*. 2004;85(18):3977–3979.
52. Kasparian J, Rodriguez M, Méjean G, Yu J, Salmon E, Wille H, Bourayou R, Frey S, Andre YB, Mysyrowicz A, et al. White-light filaments for atmospheric analysis. *Science*. 2003;301(5629):61–64.
53. Skrodzki PJ, Burger M, Finney LA, Nees J, Jovanovic I. Improved analytical performance of remote laser-induced breakdown spectroscopy via concatenation of filament-driven optical waveguides formed in air. Paper presented at: ICOPS 2022. Proceedings of the 49th IEEE International Conference on Plasma Science; 2022 May 22–26; Seattle, WA.
54. Burger M, Polynkin P, Jovanovic I. Filament-induced breakdown spectroscopy with structured beams. *Opt Express*. 2020;28(24):36812–36821.
55. Abdul Kalam S, Rao SVBM, Jayananda M, Venugopal Rao S. Standoff femtosecond filament-induced breakdown spectroscopy for classification of geological materials. *J Anal At Spectrom*. 2020;35(12):3007–3020.
56. Zhao YL, Li GG, Hou HM, Shi JC, Luo SN. CN and C_2 formation mechanisms in fs-laser induced breakdown of nitromethane in Ar or N_2 atmosphere. *J Hazard Mater*. 2020;393:Article 122396.
57. Sreedhar S, Nageswara Rao E, Manoj Kumar G, Tewari SP, Venugopal Rao S. Molecular formation dynamics of 5-nitro-2,4-dihydro-3H-1,2,4-triazol-3-one, 1,3,5-trinitroperhydro-1,3,5-triazine, and 2,4,6-trinitrotoluene in air, nitrogen, and argon atmospheres studied using femtosecond laser induced breakdown spectroscopy. *Spectrochim Acta B At Spectrosc*. 2013;87:121–129.
58. Chichkov BN, Momma C, Nolte S, Alvensleben F, Tünnermann A. Femtosecond, picosecond and nanosecond laser ablation of solids. *Appl Phys A Mater Sci Process*. 1996;63(2):109–115.
59. Wessel W, Brueckner-Foit A, Mildner J, Englert L, Haag L, Horn A, Wollenhaupt M, Baumert T. Use of femtosecond laser-induced breakdown spectroscopy (fs-LIBS) for micro-crack analysis on the surface. *Eng Fract Mech*. 2010;77(11):1874–1883.
60. Lu P, Wu J, Zeng H. Manipulation of plasma grating by impulsive molecular alignment. *Appl Phys Lett*. 2013;103(22):Article 221113.
61. Liu F, Yuan S, He B, Nan J, Khan AQ, Ding L, Zeng H. Enhanced stimulated Raman scattering by femtosecond ultraviolet plasma grating in water. *Appl Phys Lett*. 2018;112(9):Article 094101.
62. Shi L, Li W, Wang Y, Lu X, Ding L, Zeng H. Generation of high-density electrons based on plasma grating induced bragg diffraction in air. *Phys Rev Lett*. 2011;107(9):Article 095004.
63. Varma S, Chen YH, Milchberg HM. Trapping and destruction of long-range high-intensity optical filaments by molecular quantum wakes in air. *Phys Rev Lett*. 2008;101(20):Article 205001.
64. Yang X, Wu J, Peng Y, Tong Y, Lu P, Ding L, Xu Z, Zeng H. Plasma waveguide array induced by filament interaction. *Opt Lett*. 2009;34(24):3806–3808.
65. Vinçotte A, Bergé L. Femtosecond optical vortices in air. *Phys Rev Lett*. 2005;95(19):Article 193901.
66. Shih M, Segev M, Salamo G. Three-dimensional spiraling of interacting spatial solitons. *Phys Rev Lett*. 1997;78(13):2551–2554.
67. Królikowski W, Holmstrom SA. Fusion and birth of spatial solitons upon collision. *Opt Lett*. 1997;22(6):369–371.
68. Bergé L, Schmidt MR, Rasmussen JJ, Christiansen PL, Rasmussen KØ. Amalgamation of interacting light beamlets in Kerr-type media. *J Opt Soc Am B*. 1997;14(10):2550–2562.
69. Suntsov S, Abdollahpour D, Papazoglou DG, Tzortzakis S. Femtosecond laser induced plasma diffraction gratings in air as photonic devices for high intensity laser applications. *Phys Lett*. 2009;94:Article 251104.
70. Pai C-H, Huang S-Y, Kuo C-C, Lin M-W, Wang J, Chen S-Y, Lee C-H, Lin J-Y. Fabrication of spatial transient-density structures as high-field plasma photonic devices. *Phys Plasmas*. 2005;12(7):Article 070707.
71. Mohamed WTY. Improved LIBS limit of detection of Be, Mg, Si, Mn, Fe and Cu in aluminum alloy samples using a portable echelle spectrometer with ICCD camera. *Opt Laser Technol*. 2008;40(1):30–38.
72. Yaroshchyk P, Morrison RJS, Body D, Chadwick BL. Quantitative determination of wear metals in engine oils using LIBS: The use of paper substrates and a comparison between single- and double-pulse LIBS. *Spectrochim Acta B At Spectrosc*. 2005;60(11):1482–1485.
73. Zhang D, Nie J, Niu X, Chen F, Hu Z, Wen X, Li Y, Guo L. Time-resolved spectral-image laser-induced breakdown spectroscopy for precise qualitative and quantitative analysis of milk powder quality by fully excavating the matrix information. *Food Chem*. 2022;386:Article 132763.
74. Xiu J, Motto-Ros V, Panczer G, Zheng R, Yu J. Feasibility of wear metal analysis in oils with parts per million and sub-parts per million sensitivities using laser-induced breakdown spectroscopy of thin oil layer on metallic target. *Spectrochim Acta B At Spectrosc*. 2014;91:24–30.
75. Golik SS, Ilyin AA, Babiy MY, Biryukova YS, Lisitsa VV, Bukin OA. Determination of iron in water solution by time-resolved femtosecond laser-induced breakdown spectroscopy. *Plasma Sci Technol*. 2015;17(11):975–978.
76. Habermeier H-U. Pulsed laser deposition—A versatile technique only for high-temperature superconductor thin-film deposition. *Appl Surf Sci*. 1993;69(1–4):204–211.
77. Ullah F, Nguyen TK, Le CT, Kim YS. Pulsed laser deposition assisted grown continuous monolayer MoSe2. *CrystEngComm*. 2016;18(37):6992–6996.
78. Serna MI, Hasan SMN, Nam S, Bouanani LE, Moreno S, Choi H, Alshareef HN, Minary-Jolandan M, Quevedo-Lopez MA. Low-temperature deposition of layered $SnSe_2$ for heterojunction diodes. *Adv Mater Interfaces*. 2018;5(16):Article 1800128.
79. Hilmi I, Lotnyk A, Gerlach JW, Schumacher P, Rauschenbach B. Research update: Van-der-Waals epitaxy of layered chalcogenide Sb_2Te_3 thin films grown by pulsed laser deposition. *APL Mater*. 2017;5(5):Article 050701.
80. Shrivastava M, Ramgopal Rao V. A roadmap for disruptive applications and heterogeneous integration using two-

dimensional materials: State-of-the-art and technological challenges. *Nano Lett*. 2021;21(15):6359–6381.
81. Ortiz W, Malca C, Barrionuevo D, Aldalbahi A, Pacheco E, Oli N, Feng P. Two-dimensional tungsten disulfide nanosheets and their application in self-powered photodetectors with ultra-high sensitivity and stability. *Vacuum*. 2022;201:Article 111092.
82. Yao J, Zheng Z, Yang G. Layered tin monoselenide as advanced photothermal conversion materials for efficient solar energy-driven water evaporation. *Nanoscale*. 2018;10(6):2876–2886.
83. Rathod UP, Egede J, Voevodin AA, Shepherd ND. Extrinsic p-type doping of few layered WS_2 films with niobium by pulsed laser deposition. *Appl Phys Lett*. 2018;113(6): Article 062106.
84. Pelenovich VO, Xiao R, Liu Y, Liu P, Li M, He Y, Fu D. Characterization of Bi_2Se_3:Fe epitaxial films grown by pulsed laser deposition. *Thin Solid Films*. 2015;577:119–123.
85. Lin Z, Li J, Zheng Z, Li L, Yu L, Wang C, Yang G. A floating sheet for efficient photocatalytic water splitting. *Adv Energy Mater*. 2016;6(15):Article 1600510.
86. Liu JR, Bai T, Li TJ, Heng YD, Ge WL, Xiao Y, Sheng W, Sheng YX. Study on pulsed excimer laser deposited films. *High Power Laser Part Beams*. 2002;14:646–650.